Environmental Science & Technology

pubs.acs.org/est

Article

# Controllable Pyridine N-Oxidation−Nucleophilic Dechlorination Process for Enhanced Dechlorination of Chloropyridines: The Cooperation of $HCO_4^-$ and $HO_2^-$

Ying Chen, Lei Tian, Wen Liu, Yi Mei, Qiu-Ju Xing, Yi Mu, Ling-Ling Zheng, Qian Fu, Jian-Ping Zou,* and Daishe Wu*

Cite This: *Environ. Sci. Technol.* 2024, 58, 4438−4449

Read Online



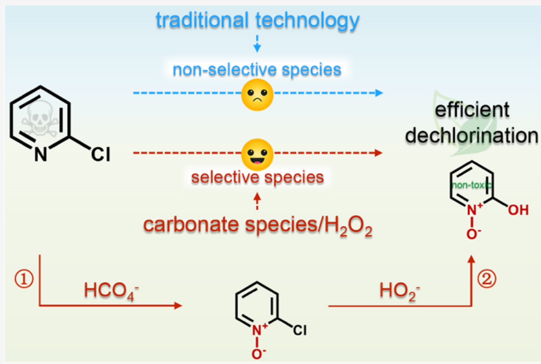


**ABSTRACT:** Dechlorination of chloropyridines can eliminate their detrimental environmental effects. However, traditional dechlorination technology cannot efficiently break the C−Cl bond of chloropyridines, which is restricted by the uncontrollable nonselective species. Hence, we propose the carbonate species-activated hydrogen peroxide (carbonate species/$H_2O_2$) process wherein the selective oxidant (peroxymonocarbonate ion, $HCO_4^-$) and selective reductant (hydroperoxide anion, $HO_2^-$) controllably coexist by manipulation of reaction pH. Taking 2-chloropyridine (Cl−Py) as an example, $HCO_4^-$ first induces Cl−Py into pyridine N-oxidation intermediates, which then suffer from the nucleophilic dechlorination by $HO_2^-$. The obtained dechlorination efficiencies in the carbonate species/$H_2O_2$ process (32.5−84.5%) based on the cooperation of $HCO_4^-$ and $HO_2^-$ are significantly higher than those in the $HO_2^-$-mediated sodium hydroxide/hydrogen peroxide process (0−43.8%). Theoretical calculations confirm that pyridine N-oxidation of Cl−Py can effectively lower the energy barrier of the dechlorination process. Moreover, the carbonate species/$H_2O_2$ process exhibits superior anti-interference performance and low electric energy consumption. Furthermore, Cl−Py is completely detoxified via the carbonate species/$H_2O_2$ process. More importantly, the carbonate species/$H_2O_2$ process is applicable for efficient dehalogenation of halogenated pyridines and pyrazines. This work offers a simple and useful strategy to enhance the dehalogenation efficiency of halogenated organics and sheds new insights into the application of the carbonate species/$H_2O_2$ process in practical environmental remediation.

**KEYWORDS:** *C−Cl bond, peroxymonocarbonate ion, hydroperoxide anion, pyridine N-oxidation, nucleophilic dechlorination*

## ■ INTRODUCTION

The excessive use of chloropyridines in agriculture planting and chemical engineering makes them ubiquitous in aquatic environments.[1,2] Although reductive dechlorination technologies have been reported to eliminate their detrimental environmental effects, these technologies require highly active catalysts and harsh reaction conditions to break the strong carbon−chlorine (C−Cl) bond.[3−5] Therefore, it is urgent to develop efficient methods for the enhanced C−Cl bond cleavage of chloropyridines.

Decreasing the electron density of the C atom in the C−Cl bond is the key factor in facilitating the reductive cleavage of the C−Cl bond.[6−8] Generally, the electrons in the C atom could be subtracted by the nearby oxidative reaction, resulting in the declined electron density of the C atom.[9,10] Moreover, previous studies have proved that the C−Cl bond in the oxidized intermediates of chlorinated organics rather than the C−Cl bond in chlorinated organics could be more easily broken in the reducing reaction.[11] Therefore, the enhanced C−Cl bond cleavage of chlorinated organics can be realized by coupling the oxidation and reduction processes. Till now, the coexistence of oxidation and reduction processes can be obtained in electrochemical systems by simultaneously generating oxidative species (hydroxyl radical ($^\bullet$OH)) and reductive species (atomic hydrogen (H*)).[12−14] However, two crucial bottlenecks restrict the improvement of dechlorination efficiencies of chlorinated organics in these systems, namely, (i) the generation of $^\bullet$OH and H* is uncontrolled[15,16] and (ii) $^\bullet$OH and H* are nonselective species, inevitably leading to the production of undesirable intermediates that decreases the dechlorination efficiency of chlorinated organics.[17−19] Thus, it

Received: November 24, 2023
Revised: January 15, 2024
Accepted: January 23, 2024
Published: February 8, 2024

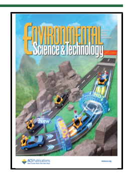

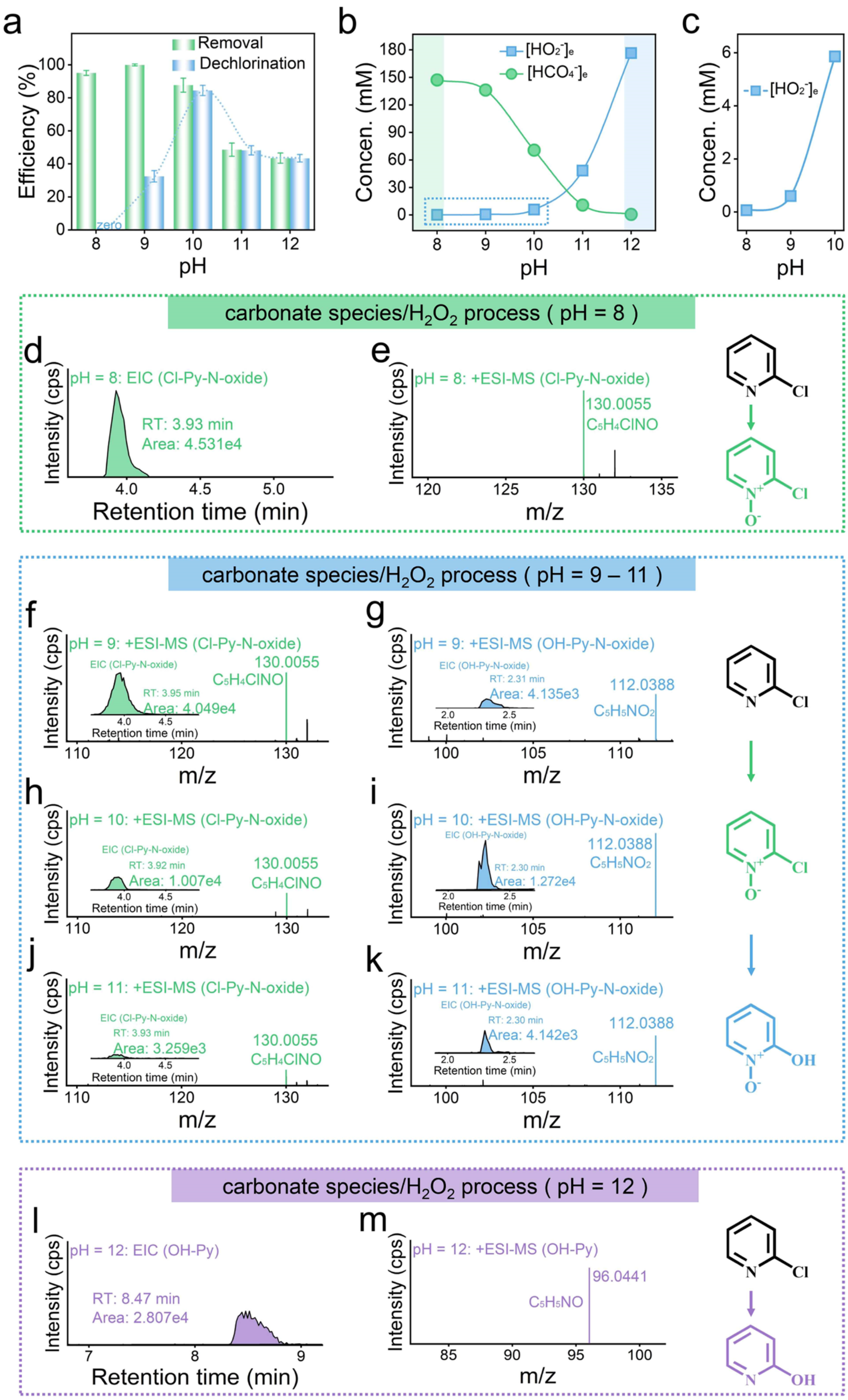


**Figure 1.** (a) Dependence of the removal efficiency and dechlorination efficiency of Cl−Py on reaction pH in the carbonate species/$H_2O_2$ process. (b) Variation of equilibrium concentrations of $HCO_4^-$ and $HO_2^-$ in the carbonate species/$H_2O_2$ process under different pH conditions. (c) The magnified view of the variation of equilibrium concentrations of $HO_2^-$ in the carbonate species/$H_2O_2$ process at pH 8.0−10.0. (d) Extracted ion chromatograms (EIC) and (e) positive electrospray ionization-mass spectrometry (+ESI-MS) of 2-chloropyridine-N-oxide (Cl−Py−N-oxide) in the carbonate species/$H_2O_2$ process at pH 8.0. EIC and + ESI-MS of (f, h, and j) Cl−Py−N-oxide and (g, i, and k) 2-hydroxypyridine N-oxide (OH−Py−N-oxide) in the carbonate species/$H_2O_2$ process at pH 9.0−11.0. (l) EIC and (m) + ESI-MS of 2-hydroxypyridine (OH−Py) in the carbonate species/$H_2O_2$ process at pH 12.0. Experimental conditions: $[Cl-Py]_0$ = 0.1 mM, $[H_2O_2]_0$ = 250 mM, $[HCO_3^-$ or $CO_3^{2-}]_0$ = 2000 mM, pH = 8.0−12.0.



https://doi.org/10.1021/acs.est.3c09878
Environ. Sci. Technol. 2024, 58, 4438−4449

is urgent to develop a novel system to controllably generate oxidant and reductant species with high selectivity for the efficient dechlorination of chloropyridines.

The peroxymonocarbonate ion ($HCO_4^-$) as a selective oxidant presents high reactivity toward compounds with electron-rich moieties (i.e., amines) via N-oxidation.[20,21] The hydroperoxide anion ($HO_2^-$) as a selective reductant induces the effective dechlorination of chlorinated N-heterocyclic aromatic compounds via nucleophilic substitution.[22,23] Note that the carbonate species-activated hydrogen peroxide (carbonate species/$H_2O_2$) process can well-controllably generate $HCO_4^-$ and $HO_2^-$ by manipulation of the reaction pH (eqs 1 and 2).[24,25] Moreover, the carbonate species/$H_2O_2$ process is deemed to be an environmentally friendly and sustainable strategy, since carbonate species and $H_2O_2$ are relatively inexpensive, nonpolluting, and recyclable.[26,27] Hence, we speculate that the carbonate species/$H_2O_2$ process could be a promising approach for high-efficient dechlorination of chloropyridines via coupling of pyridine N-oxidation and nucleophilic dechlorination in the coexistence of $HCO_4^-$ and $HO_2^-$.

$$H_2O_2 + HCO_3^- \rightarrow HCO_4^- + H_2O \quad K_{eq} = 0.33\ M^{-1} \tag{1}$$

$$H_2O_2 + OH^- \rightarrow HO_2^- + H_2O \quad pKa = 11.62 \tag{2}$$

In this study, in order to confirm this assumption, we selected 2-chloropyridine (Cl−Py) as a representative contaminant to investigate well the cooperation of $HCO_4^-$ and $HO_2^-$ in the carbonate species/$H_2O_2$ for effective dechlorination of Cl−Py via experiments and theoretical calculations. In addition, the superiorities of the carbonate species/$H_2O_2$ process in terms of electric energy consumption, toxicity assessment, and practical application were further evaluated in detail. Overall, this present work provides a new strategy for the enhanced dechlorination of chlorinated organics.

## ■ EXPERIMENTAL SECTION

**Chemicals and Reagents.** 2-Chloropyridine (Cl−Py, 98% purity), 2-hydroxypyridine (OH−Py, 97% purity), 2-hydroxypyridine N-oxide (OH−Py−N-oxide, 98% purity), 2-fluoropyridine (F−Py, 99% purity), 2-bromopyridine (Br−Py, 98% purity), and 2-iodopyridine (I−Py, 97% purity) were purchased from Aladdin Chemical Co., Ltd., China. Details of the other chemicals and reagents used in this study are provided in Text S1 in the Supporting Information. All of the chemicals were of reagent grade and used without further purification. The experimental solutions used in this study were all prepared with Milli-Q ultrapure water (with a specific conductivity of >18.2 MΩ cm). The strain used for toxicity testing was *Vibrio qinghaiensis sp.-Q67* from the Department of Biology at East China Normal University.[28] The real Cl−Py wastewater was collected from a company in Jiangxi Province (Cl−Py: 31.4 mg $L^{-1}$, $NO_3^-$: 75.5 mg $L^{-1}$, $NH_4^+$: 12.0 mg $L^{-1}$, $Cl^-$: 21.6 mg $L^{-1}$, COD: 212.5 mg $L^{-1}$, pH = 8.4).

**Experimental Procedure.** The batch degradation experiments were conducted in 250 mL glass bottles with a magnetic stirrer at room temperature. The initial concentration of Cl−Py or selected halogenated contaminants in the working solution was 0.1 mM. Bicarbonate ($HCO_3^-$) was used as the catalyst for carbonate species/$H_2O_2$ experiments performed at pH 8.0−9.0, while carbonate ($CO_3^{2-}$) was used as the catalyst for the experiments performed at pH 10.0−12.0. Typically, each 200 mL working solution containing the target contaminant and determined concentration of the catalyst ($HCO_3^-$ or $CO_3^{2-}$) was prepared and adjusted to the desired pH value. Then, the desired concentration of the oxidant ($H_2O_2$) was added to initiate the reaction. No buffer was used for batch degradation experiments, and the solution pH was adjusted with NaOH and $HClO_4$ and kept constant during the reaction. Periodically, 2.0 mL of the sample was collected, immediately quenched using $H_2SO_4$ stock solution (0.1 M), and then filtered (0.22 $\mu$m nylon filter membranes) before the analysis of the target contaminant. All experiments were performed in duplicate or triplicate, and the obtained average values with standard deviations were presented.

**Analytical Methods.** The concentrations of target contaminants in the samples taken from batch degradation experiments were determined with ultrahigh-performance liquid chromatography (UHPLC, Dionex, Ultimate 3000), and the details are summarized in Text S2 in the Supporting Information. The solution pH was measured by a pH meter (Mettler Toledo, FE28). The released halogen ion concentration in the filtered aqueous sample was measured by ion chromatography (Shine, CIC-D120). Equilibrium acid−base speciation of carbonate species was calculated using Visual MINTEQ. 3.1 software. The generation of $HCO_4^-$ in the carbonate species/$H_2O_2$ process was identified by $^{13}C$ nuclear magnetic resonance (NMR) spectral analysis (more details are provided in Text S3 in the Supporting Information). The absence of residual $H_2O_2$ was measured by the colorimetric cerium method.[29] The analytic methods for assessing dehalogenation efficiency, equilibrium concentrations of $HO_2^-$ and $HCO_4^-$, electron spin resonance (ESR) analysis, degradation intermediates and products, electric energy consumption, and toxicity assessment of Cl−Py and its intermediates and products are presented in Texts S4−S10 in the Supporting Information.

**Theoretical Calculation.** The geometries of reactants were optimized at the Lee−Yang−Parr gradient-corrected correlation functional (B3LYP) hybrid functional[30,31] with Grimme's DFT-D3(BJ) empirical dispersion correction[32] and the def2-TZVP[33,34] basis set level using the Gaussian 09 D.01 quantum chemical package. More details on density functional theory (DFT) calculations (including transition states, vibrational frequency calculations, Gibbs free energy of reaction, electrostatic potential (ESP) distribution, and Bader charge analysis) are shown in Text S11 in the Supporting Information.

## ■ RESULTS AND DISCUSSION

**Dechlorination Performance of Cl−Py in the Carbonate Species/$H_2O_2$ Process.** The initial molar ratio of carbonate species to $H_2O_2$ ([carbonate species]$_0$/[$H_2O_2$]$_0$) and reaction pH are the key parameters in the carbonate species/$H_2O_2$ process. In the carbonate species/$H_2O_2$ process at pH 8.0, the removal efficiency of Cl−Py increased progressively from 8.6 to 95.1% with increasing [carbonate species]$_0$/[$H_2O_2$]$_0$ (i.e., [$HCO_3^-$]$_0$/[$H_2O_2$]$_0$) from 0.2 to 8 (Figure S1). The initial molar ratio of carbonate species to $H_2O_2$ of 8 was chosen as the operating parameter for the following experiments. The influence of the reaction pH on Cl−Py removal was further investigated systematically. As shown in Figures S2 and 1a, 87.7−100% removal of Cl−Py was obtained at pH 8.0−10.0. However, a further increase in pH


https://doi.org/10.1021/acs.est.3c09878
Environ. Sci. Technol. 2024, 58, 4438−4449

(11.0−12.0) led to the decrease of the removal efficiency of Cl−Py (43.5−48.6%). These results indicate that Cl−Py can be removed in the carbonate species/$H_2O_2$ process at pH 8.0−12.0, but the removal efficiency of Cl−Py is affected by reaction pH. We further investigated the corresponding dechlorination efficiency of Cl−Py in the carbonate species/$H_2O_2$ process under different pH conditions by monitoring the released $Cl^-$ concentration. As shown in Figure S3, $Cl^-$ was not detected at pH 8.0, and the concentration of released $Cl^-$ gradually increased during the degradation of Cl−Py at pH 9.0−12.0. Figure 1a reveals the dechlorination efficiency of Cl−Py as a function of reaction pH, showing a near-volcano-shaped curve with the maximum dechlorination efficiency at pH 10.0. These results suggest that Cl−Py can be dechlorinated in the carbonate species/$H_2O_2$ process at pH 9.0−12.0, and the dechlorination efficiencies of Cl−Py at pH 10.0−12.0 (43.4−84.5%) are higher than those at pH 8.0−9.0 (0−32.5%). Considering that the generation of reactive species (including $HCO_4^-$ and $HO_2^-$) in the carbonate species/$H_2O_2$ process is controlled by the reaction pH, the difference in reactive species under different pH conditions is thereafter investigated.

As shown in Figure S4, the additional peak in the $^{13}C$ NMR spectrum at 158.9 ppm is assigned to $HCO_4^-$ besides the peaks at 161.4−168.8 ppm for $HCO_3^-$ and $CO_3^{2-}$.[35,36] Thus, the generation of $HCO_4^-$ in the carbonate species/$H_2O_2$ process at pH 8.0−11.0 is confirmed by $^{13}C$ NMR spectral analysis. Figure 1b further displays the pH-dependent variation in the equilibrium concentrations of $HCO_4^-$ and $HO_2^-$ ($[HCO_4^-]_e$ and $[HO_2^-]_e$) in the carbonate species/$H_2O_2$ process. When the pH is 8.0, $[HCO_4^-]_e$ reaches its maximum value of 147.09 mM due to the highest proportion of $HCO_3^-$ in total C-containing species (Figure S5), while $[HO_2^-]_e$ is negligible (0.06 mM). The result could well explain the observed excellent Cl−Py removal efficiency (95.1%) but no dechlorination activity in the carbonate species/$H_2O_2$ process at pH 8.0. When pH increases from 8.0 to 9.0−10.0, $[HCO_4^-]_e$ progressively decreases due to the decrease in the amount of $HCO_3^-$, whereas $[HO_2^-]_e$ dramatically increases with the increase in pH value (Figure 1c). The dechlorination efficiency of Cl−Py in the carbonate species/$H_2O_2$ process (pH 9.0−10.0) reaches as high as 32.5−84.5%. The dechlorination performance of Cl−Py by $HO_2^-$ alone is examined in the sodium hydroxide/hydrogen peroxide process (i.e., $HO_2^-$-mediated $OH^-/H_2O_2$ process). As shown in Figure S6, Cl−Py could not be degraded in the $OH^-/H_2O_2$ process at pH 9.0−10.0. These results suggest that the cooperation of $HCO_4^-$ and $HO_2^-$ in the carbonate species/$H_2O_2$ process (pH 9.0−10.0) could contribute to the enhanced dechlorination of Cl−Py. When pH increases to 11.0, $[HCO_4^-]_e$ continues to decrease, and $[HO_2^-]_e$ continues to increase and exceed $[HCO_4^-]_e$. The decrease in the dechlorination efficiency of Cl−Py at pH 11.0 shows the beneficial effect of $HCO_4^-$ on the dechlorination reaction of Cl−Py. Note that the dechlorination efficiency of Cl−Py (48.2%) in the carbonate species/$H_2O_2$ process at pH 11.0 is still higher than that (14.1%) in the $HO_2^-$-mediated $OH^-/H_2O_2$ process at pH 11.0. When pH further increases to 12.0, $[HCO_4^-]_e$ is very small (0.59 mM), whereas $[HO_2^-]_e$ reaches up to 176.45 mM. Note that there is no difference in Cl−Py dechlorination efficiency between the carbonate species/$H_2O_2$ process and the $OH^-/H_2O_2$ process at pH 12.0, revealing the negligible contribution of $HCO_4^-$ for Cl−Py dechlorination.

In addition, as shown in Figure S7, quenching experiments involving different scavengers exclude the influence of other active species (such as $^{\bullet}OH$, carbonate radical anion ($CO_3^{\bullet-}$), superoxide radical ($O_2^{\bullet-}$), and singlet oxygen ($^1O_2$)), as indicated by eqs 3−6,for Cl−Py removal in the carbonate species/$H_2O_2$ process under different pH conditions.[37] Moreover, no obvious ESR signals of active species spin-trapped by 5,5-dimethyl-1-pyrroline N-oxide (DMPO) or 2,2,6,6-tetramethylpiperidine (TEMP) were detected in the carbonate species/$H_2O_2$ process at pH 10.0 (Figure S8). These results verify no generation of active species in the carbonate species/$H_2O_2$ process.[35,38] In conclusion, the carbonate species/$H_2O_2$ processes at pH 8.0 and 12.0 are referred to as the $HCO_4^-$-mediated oxidation process and $HO_2^-$-mediated dechlorination process, respectively, while the carbonate species/$H_2O_2$ process at pH 9.0−11.0 is referred to as the $HCO_4^-$ and $HO_2^-$ co-mediated process. The aforementioned results powerfully support that the carbonate species/$H_2O_2$ process can improve the dechlorination efficiency of Cl−Py via the controllable cooperation of $HCO_4^-$ and $HO_2^-$ at pH 9.0−11.0.

$$HCO_4^- \rightarrow CO_3^{\bullet -} + ^{\bullet}OH \tag{3}$$

$$CO_3^{\bullet -} + H_2O_2 \rightarrow HCO_3^- + HO_2^{\bullet} \tag{4}$$

$$HO_2^{\bullet} \rightarrow O_2^{\bullet -} + H^+ pKa = 4.8 \tag{5}$$

$$HO_2^{\bullet} + HO_2^{\bullet} \rightarrow {}^1O_2 + H_2O_2 \tag{6}$$

To further verify these analyses, the detection of degradation intermediates and products of Cl−Py in the carbonate species/$H_2O_2$ process under different pH conditions was performed by LC-MS analysis. As shown in Figure 1d,e, only the pyridine N-oxidation product of Cl−Py (Cl−Py−N-oxide ([$C_5H_4ClNO$ + $H^+$], $m/z$ = 130.0055)) was detected in the carbonate species/$H_2O_2$ process at pH 8.0, while no dechlorination product was detected. The EIC peak area of Cl−Py−N-oxide gradually increased with the reaction time (Figure S9). The accumulation of Cl−Py−N-oxide was further quantified with an external standard calibration method. As presented in Figure S10, the concentration of Cl−Py−N-oxide was negatively correlated with Cl−Py degradation, and the conversion rate of Cl−Py to Cl−Py−N-oxide was maintained at 94.3−98.6%. These results affirmed that $HCO_4^-$ could achieve the efficient pyridine N-oxidation of Cl−Py. In the carbonate species/$H_2O_2$ process at pH 9.0−11.0, Cl−Py−N-oxide and the dechlorination product (OH−Py−N-oxide, [$C_5H_5NO_2$ + $H^+$], $m/z$ = 112.0388) were detected (Figure 1f−k). The change in the EIC of Cl−Py−N-oxide and OH−Py−N-oxide in the carbonate species/$H_2O_2$ process at pH 9.0−11.0 is shown in Figures S11−S13. We found that the EIC peak area of Cl−Py−N-oxide in the carbonate species/$H_2O_2$ process at pH 9.0 was larger than those in the carbonate species/$H_2O_2$ process at pH 10.0−11.0. The EIC peak area of OH−Py−N-oxide in the carbonate species/$H_2O_2$ process at pH 10.0 was larger than those in the carbonate species/$H_2O_2$ process at pH 9.0 and 11.0. The observation was in accordance with the aforementioned degradation and dechlorination performances of Cl−Py. To further observe the dynamic changes of products during the reaction, the concentration−time curves of Cl−Py, Cl−Py−N-oxide, and OH−Py−N-oxide are shown in Figure S14. As the reaction time increased, the concentration of Cl−Py gradually decreased, and Cl−Py−N-oxide was generated and then consumed while the concentration of OH−Py−N-



https://doi.org/10.1021/acs.est.3c09878
Environ. Sci. Technol. 2024, 58, 4438−4449

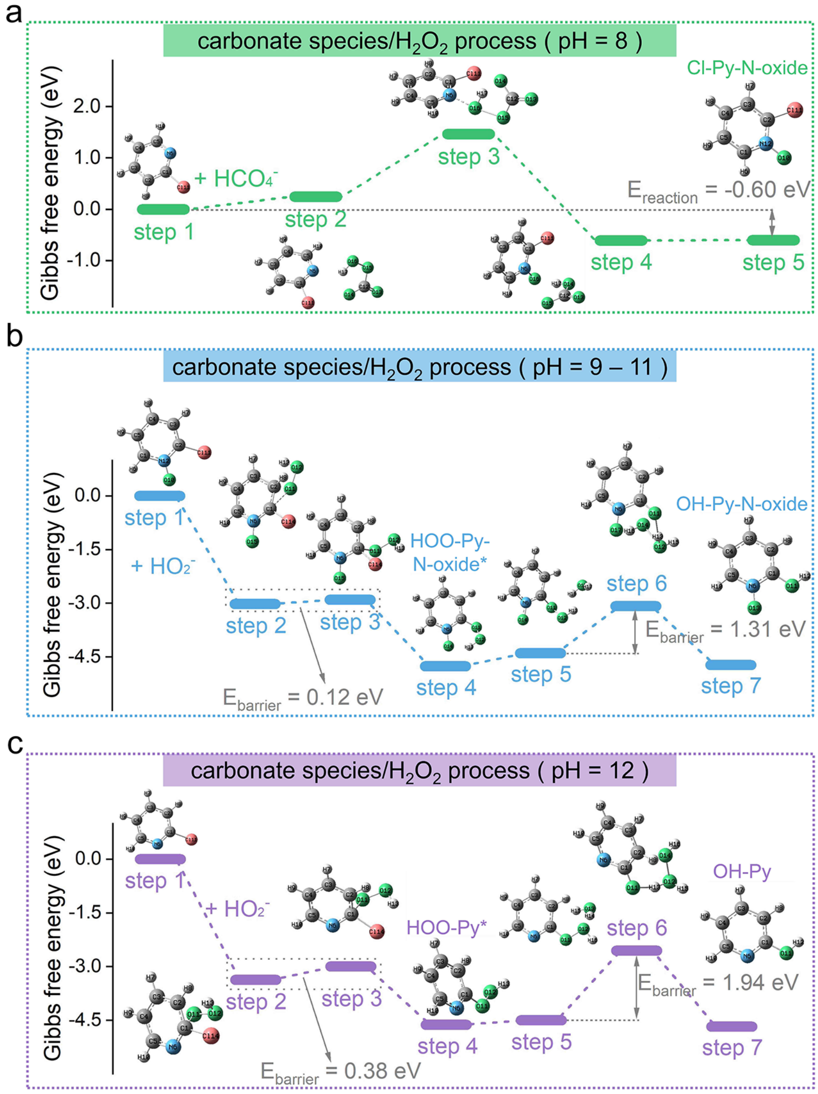


**Figure 2.** Gibbs free energy profiles of (a) pyridine N-oxidation of Cl−Py, (b) dechlorination−hydroxylation of Cl−Py−N-oxide, and (c) dechlorination−hydroxylation of Cl−Py in the carbonate species/$H_2O_2$ process.

oxide kept increasing. These results provided solid evidence for the cooperation of $HCO_4^-$ and $HO_2^-$ in facilitating Cl−Py dechlorination, wherein $HCO_4^-$ initiated the pyridine N-oxidation of Cl−Py and $HO_2^-$ promoted nucleophilic dechlorination of the generated N-oxidation intermediate (Cl−Py−N-oxide). Moreover, OH−Py ([$C_5H_5NO$ + $H^+$], $m/z$ = 96.0441) was found in the carbonate species/$H_2O_2$ process at pH 11.0 (Figure S15). The finding implied that adequate $HO_2^-$-initiated the dechlorination−hydroxylation of Cl−Py at pH 11.0. As shown in Figure 1l,m, OH−Py as the only product was detected in the carbonate species/$H_2O_2$ process at pH 12.0, further indicating the contribution of $HO_2^-$ alone for the dechlorination−hydroxylation of Cl−Py. The above results confirm that the enhanced dechlorination of Cl−Py in the carbonate species/$H_2O_2$ process is associated with the $HCO_4^-$ and $HO_2^-$ co-mediated pyridine N-oxidation−nucleophilic dechlorination coupling reaction.

**Mechanism of Cl−Py Removal in the Carbonate Species/$H_2O_2$ Process.** We conduct DFT calculations to further analyze and compare the theoretical pathways of Cl−Py removal in the carbonate species/$H_2O_2$ process under different pH conditions. It is widely known that $HCO_4^-$ is a selective oxidant (i.e., selective electrophile).[23,24] As shown in Figures 2a and S16, in the carbonate species/$H_2O_2$ process at pH 8.0, the pyridine N-oxidation of Cl−Py by $HCO_4^-$ is achieved by the nucleophilic attack of pyridine N at the electrophilic oxygen (O16) of $HCO_4^-$.[39,40] The negative Gibbs free energy change (−0.60 eV) of this reaction indicates that $HCO_4^-$-mediated pyridine N-oxidation of Cl−Py is thermodynamically spontaneous, which is consistent with the efficient pyridine N-oxidation performance of Cl−Py at pH 8.0.

In the carbonate species/$H_2O_2$ process at pH 9.0−11.0, Cl−Py is first oxidized by $HCO_4^-$ to form Cl−Py−N-oxide. It is widely known that $HO_2^-$ is a selective reductant (i.e., nucleophile).[22,41] The terminal O atom in $HO_2^-$ with nonbonding electron pairs can nucleophilically attack the C atom of the C−Cl bond in chlorinated organics via a Meisenheimer intermediate, resulting in the decomposition of the C−Cl bond and the formation of an intermediate containing an O−OH bond (i.e., nucleophilic substitution process).[42−45] As shown in Figures 2b and S17, the nucleophilic attack of $HO_2^-$ on Cl−Py−N-oxide occurs via a Meisenheimer intermediate (step 3), leading to the generation of a dechlorination intermediate (hydroperoxide-substituted


https://doi.org/10.1021/acs.est.3c09878
Environ. Sci. Technol. 2024, 58, 4438−4449

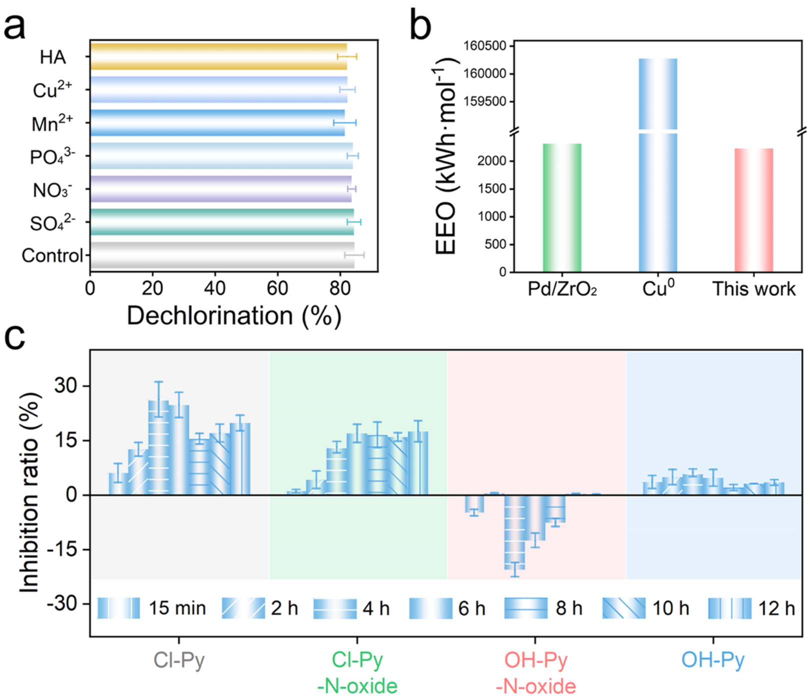


**Figure 3.** (a) Influence of coexisting substances on Cl−Py dechlorination in the carbonate species/$H_2O_2$ process. (b) Comparison of energy consumption in different processes. (c) Toxicity assessment of Cl−Py and its degradation intermediates and products. Experimental conditions: $[Cl-Py]_0$ = 0.1 mM, $[H_2O_2]_0$ = 250 mM, $[CO_3^{2-}]_0$ = 2000 mM, [coexisting ions]$_0$ = 1 mM, $[HA]_0$ = 10 mg $L^{-1}$, pH = 10.0.

pyridine N-oxide (HOO−Py−N-oxide*)) containing an O−OH bond. Moreover, the reaction process is supported by the detection of HOO−Py−N-oxide ($[C_5H_5NO_3-H^+]$, $m/z$ = 126.0195; Figure S18). The calculated energy barrier for the nucleophilic substitution reaction between $HO_2^-$ and Cl−Py−N-oxide is 0.12 eV. In the following steps (steps 5−7), HOO−Py−N-oxide* undergoes hydrolysis to release $H_2O_2$ and forms the final hydroxylation product (OH−Py−N-oxide).[41] These results elucidate that $HO_2^-$ induces the C−Cl bond of Cl−Py to the C−OH bond via coupling reactions of nucleophilic substitution and hydrolyzation, which is different from H*-induced hydrogenolysis of the C−Cl bond (i.e., C−Cl bond to C−H bond).[4,5]

In the carbonate species/$H_2O_2$ process at pH 12.0, the nucleophilic substitution reaction between Cl−Py and $HO_2^-$ is difficult to achieve due to the high energy barrier (0.38 eV; Figures 2c and S19). To gain insights into the difference between Cl−Py and Cl−Py−N-oxide, a comparative analysis of ESP analysis between Cl−Py and Cl−Py−N-oxide is given in Figure S20. Compared with the C−Cl bond of Cl−Py with negative ESP (−1.45 kcal $mol^{-1}$), the C−Cl bond in Cl−Py−N-oxide possesses a positive ESP value (5.66 kcal $mol^{-1}$), demonstrating that Cl−Py−N-oxide rather than Cl−Py is more amenable to nucleophilic attack for promoting the dechlorination process. Moreover, the further comparative analysis of the Bader charge between Cl−Py and Cl−Py−N-oxide reveals that the charge of the 1C atom of the C−Cl bond in Cl−Py−N-oxide (0.671333 e) is more positive than that of the 1C atom of the C−Cl bond in Cl−Py (0.611253 e; Table S1). The result testifies that pyridine N-oxidation of Cl−Py leads to the declined electron density of the C atom in the C−Cl bond. Furthermore, in the $HO_2^-$-mediated $OH^-/H_2O_2$ process at pH 9.0−12.0, the dechlorination efficiencies of Cl−Py−N-oxide (24.2−92.8%) were considerably higher than those of Cl−Py (0−44.1%), providing the direct evidence that Cl−Py−N-oxide rather than Cl−Py is more easily and rapidly dechlorinated by $HO_2^-$ alone (Figure S21). Additionally, note that the energy barrier for the subsequent hydrolysis process of the generated hydroperoxide-substituted pyridine (HOO−Py*) is 1.5 times higher than that for the hydrolysis of HOO−Py−N-oxide*. Thus, $HO_2^-$ alone-initiated dechlorination−hydroxylation of Cl−Py is limited by the high reaction energy barrier, which is consistent with the inefficient dechlorination efficiency of Cl−Py in the $HO_2^-$-mediated $OH^-/H_2O_2$ process. Therefore, these results highlight that the carbonate species/$H_2O_2$ process based on the cooperation of $HCO_4^-$ and $HO_2^-$ can significantly promote the dechlorination of Cl−Py via lowering the reaction energy barrier.

**Application Potential.** Given that inorganic salt ions and humic acid (HA) are typically present in real wastewater environments, it is necessary to check whether these coexisting substances could affect the dechlorination efficiency of Cl−Py in the carbonate species/$H_2O_2$ process. Considering the dechlorination performances of Cl−Py under different pH conditions, the carbonate species/$H_2O_2$ process at pH 10.0 was chosen as the performing condition in the following experiments. As shown in Figure 3a, in the presence of $SO_4^{2-}$, $NO_3^-$, and $PO_4^{3-}$, there was no distinct difference among the dechlorination efficiencies of Cl−Py. The finding could be because the reactive species ($HCO_4^-$ and $HO_2^-$) with high selectivity are less affected by the water matrices than traditional radicals.[46,47] However, after the addition of $Mn^{2+}$ and $Cu^{2+}$, the dechlorination efficiencies of Cl−Py slightly decreased to 81.4 and 82.3%, respectively. This result could be explained by the fact that metal ions ($M^{n+}$) induce the competing reaction with Cl−Py dechlorination by utilizing carbonate species and $H_2O_2$ (eqs 7 and 8).[21] In the presence of HA, the dechlorination efficiency of Cl−Py reached about 82%, which was slightly lower than that in the carbonate species/$H_2O_2$ process without the addition of any chemical


https://doi.org/10.1021/acs.est.3c09878
Environ. Sci. Technol. 2024, 58, 4438−4449

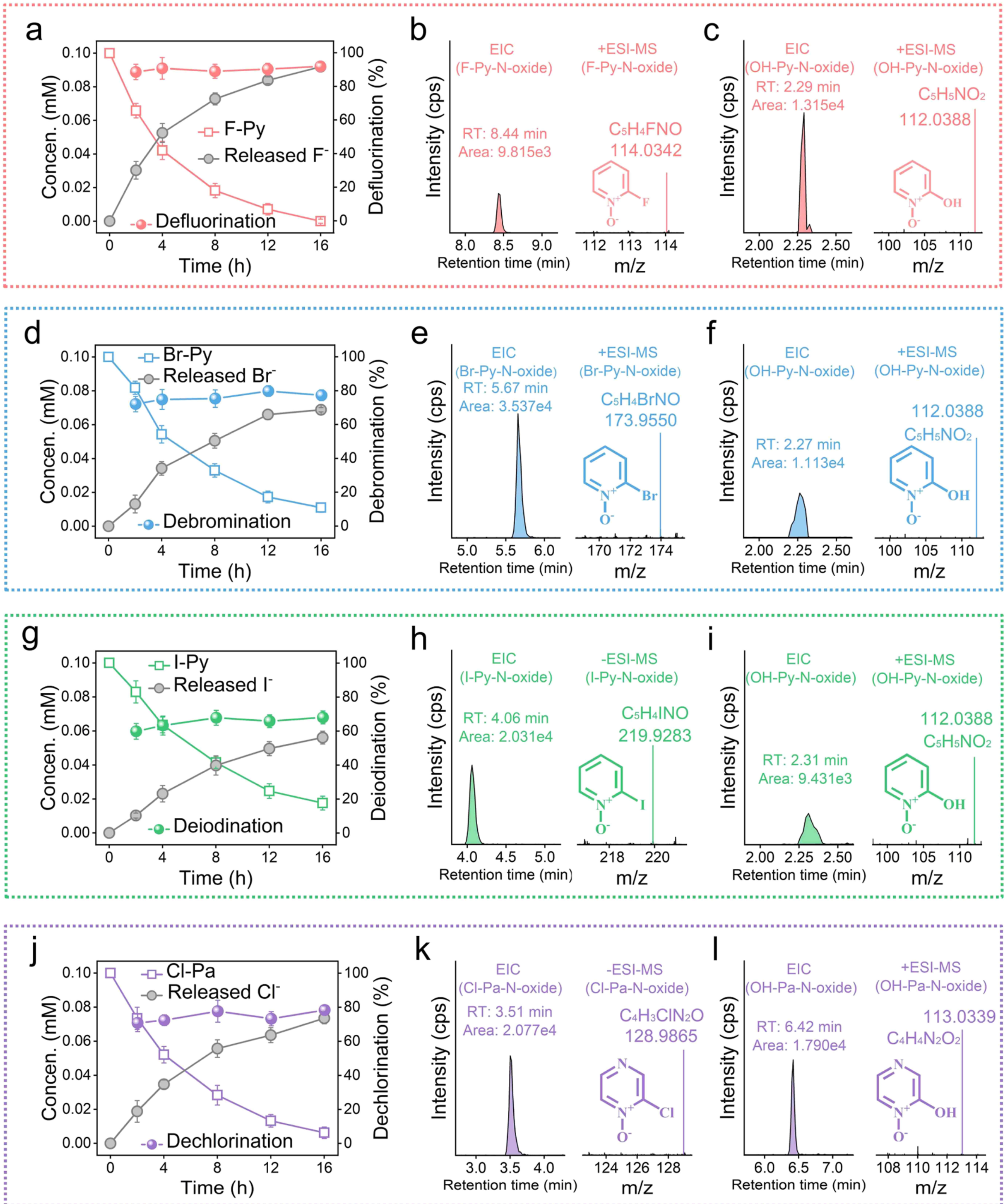


**Figure 4.** (a) Defluorination performance, (b) degradation intermediate, and (c) product of F−Py in the carbonate species/$H_2O_2$ process; (d) debromination performance, (e) degradation intermediate, and (f) product of Br−Py in the carbonate species/$H_2O_2$ process; (g) deiodination performance, (h) degradation intermediate, and (i) product of I−Py in the carbonate species/$H_2O_2$ process; (j) dechlorination performance, (k) degradation intermediate, and (l) product of Cl−Pa in the carbonate species/$H_2O_2$ process. Experimental conditions: [halogenated pyridines]$_0$ = [Cl−Pa]$_0$ = 0.1 mM, [$H_2O_2$]$_0$ = 250 mM, [$CO_3^{2-}$]$_0$ = 2000 mM, pH = 10.0.

reagent (84.5%). The phenomenon could be related to the competitive consumption of reactive species by the aromatic rings and oxygen-bearing functional groups of humic acid.[48,49] We applied the carbonate species/$H_2O_2$ process to treat real


https://doi.org/10.1021/acs.est.3c09878
Environ. Sci. Technol. 2024, 58, 4438−4449

Cl−Py wastewater. As shown in Figure S22, the concentration of Cl−Py decreased from 31.4 mg to 1.8 mg $L^{-1}$ within 48 h. Moreover, the increased $Cl^-$ concentration was detected after 48 h of the reaction (Figure S23). Thus, these results demonstrate the great potential of the carbonate species/$H_2O_2$ process in treating practical wastewater.

$$M^{n+}(HCO_3^-)_n + HO_2^- + (4-n)HCO_3^- \rightarrow M^{n+1}(HCO_3^-)_3 + 2OH^- + CO_3^{\bullet -} \quad (7)$$

$$M^{n+1}(HCO_3^-)_3 + HO_2^- + OH^- \rightarrow M^{n+}(HCO_3^-)_n + O_2^{\bullet -} + (3-n)HCO_3^- + H_2O \quad (8)$$

To evaluate the economic efficiency of the carbonate species/$H_2O_2$ process, the electric energy consumption of an additional experiment (the reaction volume of 1 L) was determined. The electronic energy equivalent of 1 mol of $Na_2CO_3$ (industrial grade, 20 $/metric ton) and liquid $H_2O_2$ (industrial grade, 500 $/metric ton) are converted to 0.01 and 0.81 kWh, respectively, as previously reported.[28] The corresponding electric energy consumption was calculated to be 2230.0 kWh $mol^{-1}$ when the dechlorination efficiency of Cl−Py was 100% in the carbonate species/$H_2O_2$ process (Figures S24 and 3b). For comparison, the electric energy consumptions of other reported processes for Cl−Py dechlorination (such as zirconia-supported palladium catalyst-mediated liquid-phase hydrodechlorination (Pd/$ZrO_2$-mediated HDC) and zerovalent copper-mediated catalytic hydrodechlorination ($Cu^0$-mediated HDC)) were derived from previous studies (Table S2).[50,51] We find that the electric energy consumption of the carbonate species/$H_2O_2$ process for Cl−Py dechlorination is lower than that of Pd/$ZrO_2$-mediated HDC (2315.6 kWh $mol^{-1}$). Moreover, the electric energy consumption of the carbonate species/$H_2O_2$ process for Cl−Py dechlorination is 2 orders of magnitude less than that of the $Cu^0$-mediated HDC (160277.9 kWh $mol^{-1}$). In the carbonate species/$H_2O_2$ process, the concentration of $H_2O_2$ was not significantly changed before and after the reaction (Figure S25). The residual $H_2O_2$ at high concentrations can continue to be used for wastewater treatment. Thus, these results verify that the carbonate species/$H_2O_2$ process is more sustainable and economically viable than other processes for Cl−Py dechlorination.

To investigate the toxicity changes of Cl−Py transformation in the carbonate species/$H_2O_2$ process, the acute ($LC_{50}$ and $EC_{50}$) and chronic toxicities (ChV) of Cl−Py and its degradation intermediates/products (including Cl−Py−N-oxide and OH−Py−N-oxide) to different species (i.e., fish, daphnid, and green algae) were predicted by the Ecological Structure−Activity Relationships (ECOSAR) program. As presented in Table S3, Cl−Py−N-oxide exhibited lower acute and chronic toxicity compared to very toxic Cl−Py, which was classified as toxic to aquatic organisms (1 mg $L^{-1}$ < $LC_{50}/EC_{50}$/ChV ≤ 10 mg $L^{-1}$).[52] Note that OH−Py−N-oxide was classified as not harmful to aquatic organisms ($LC_{50}/EC_{50}$/ChV greater than 100 mg $L^{-1}$), demonstrating that the complete detoxification of Cl−Py could be achieved in the carbonate species/$H_2O_2$ process.[53] Comparatively, the toxicity of OH−Py produced by the $HO_2^-$-mediated $OH^-/H_2O_2$ process was found in the category of harmful (10 mg $L^{-1}$ < $LC_{50}/EC_{50}$/ChV ≤ 100 mg $L^{-1}$). The strain *Vibrio qinghaiensis sp.-Q67* is a sensitive model for assessing the acute toxicity of chemicals.[54,55] To further check the aforementioned results, the *Vibrio qinghaiensis sp.-Q67* luminescence inhibition test was performed to experimentally evaluate the ecotoxicity of Cl−Py and its degradation intermediates and products. As shown in Figure 3c, the inhibition effect of Cl−Py−N-oxide on *Vibrio qinghaiensis sp.-Q67* (1.1−17.5%) was lower than that of Cl−Py (6.1−26.3%). OH−Py−N-oxide showed luminescence promotion on *Vibrio qinghaiensis sp.-Q67*, implying its nontoxicity. 2.1−6.1% of luminescence inhibition was obtained in the presence of OH−Py. These observations are in agreement with the predicted toxicity results. In addition, it was observed that the reduction products of Cl−Py (such as pyridine and piperidine) in the traditional reductive technologies exhibited higher acute and chronic toxicity than OH−Py−N-oxide (Table S3).[50,51,56] The above results demonstrate that the carbonate species/$H_2O_2$ process is an efficient strategy for the complete detoxification of Cl−Py.

**Dehalogenation of Halogenated Pyridines and Pyrazines.** First, we explored the degradation of halogenated pyridines by $HO_2^-$ alone. As shown in Figure S26, halogenated pyridines could not be degraded in the $HO_2^-$-mediated $OH^-/H_2O_2$ process at pH 10.0. As shown in Figure 4a, the carbonate species/$H_2O_2$ process realized 100% F−Py removal within 16 h. Moreover, the released $F^-$ concentration continuously increased with F−Py removal, and the corresponding defluorination efficiency reached 88.5−91.9%. Furthermore, pyridine N-oxidation intermediates (F−Py−N-oxide, [$C_5H_4FNO$ + $H^+$], $m/z$ = 114.0342) and the final defluorination product (OH−Py−N-oxide) of F−Py were detected (Figure 4b,c). These findings manifest that the carbonate species/$H_2O_2$ process could achieve defluorination of F−Py via the pyridine N-oxidation−nucleophilic defluorination coupling pathway. As for Br−Py, 89.0% removal efficiency and 77.3% debromination efficiency were obtained in the carbonate species/$H_2O_2$ process (Figure 4d). The pyridine N-oxidation intermediates (Br−Py−N-oxide, [$C_5H_4BrNO$ + $H^+$], $m/z$ = 173.9550) and the final debromination product (OH−Py−N-oxide) of Br−Py were also identified, proving the ability of the carbonate species/$H_2O_2$ process for pyridine N-oxidation−nucleophilic debromination of Br−Py (Figure 4e,f). Additionally, 82.5% of I−Py was degraded in the carbonate species/$H_2O_2$ process (Figure 4g). The released $I^-$ from I−Py within 16 h was 0.06 mM, indicating the corresponding 68% deiodination. 2-Iodopyridine-N-oxide (I−Py−N-oxide, [$C_5H_4INO$ - $H^+$], $m/z$ = 219.9283) and OH−Py−N-oxide was observed during degradation of I−Py (Figure 4h,i). Note that the dehalogenation efficiency of halogenated pyridines in the carbonate species/$H_2O_2$ process is in the order F−Py > Br−Py > I−Py. Considering that the dehalogenation efficiency of halogenated pyridines is related to pyridine N-oxidation and nucleophilic substitution processes. First, the influence of halogen species in halogenated pyridines on the pyridine N-oxidation process is investigated in the carbonate species/$H_2O_2$ process at pH 8.0. As shown in Figure S27, the difference in the halogen species of halogenated pyridines had little effect on the pyridine N-oxidation of halogenated pyridines. Thus, the difference in the dehalogenation efficiency of halogenated pyridines is ascribed to $HO_2^-$-mediated nucleophilic substitution. Note that the reaction rate of nucleophilic substitution is positively associated with the electron-deficient nature of the C atom in the C−X bond (X = F, Cl, Br, I).[57,58] The highest electron-


https://doi.org/10.1021/acs.est.3c09878
*Environ. Sci. Technol.* 2024, 58, 4438−4449

withdrawing effect from F results in the most electron-deficient carbon atom, which is most prone to nucleophilic attack.[59,60] Moreover, it has been reported that $HO_2^-$ can nucleophilically attack electron-deficient carbon atoms of perfluorooctanoic acid (PFOA), achieving defluorination of PFOA. This can explain why the defluorination efficiency of F−Py is higher than the dehalogenation efficiency of Br−Py and I−Py in the carbonate species/$H_2O_2$ process.

Additionally, the carbonate species/$H_2O_2$ process achieved 93.8% removal efficiency as well as 78.4% dechlorination efficiency of 2-chlorpyrazine (Cl−Pa; Figure 4j). 2-Chlorpyrazine-N-oxide (Cl−Pa−N-oxide, $[C_4H_3ClN_2O - H^+]$, $m/z$ = 128.9865) and hydroxypyrazine-N-oxide (OH−Pa−N-oxide, $[C_4H_4N_2O_2 + H^+]$, $m/z$ = 113.0339) were detected to be the pyrazine N-oxidation intermediate and the final dechlorination product of Cl−Pa, respectively (Figure 4k,l). The phenomenon further demonstrates that the carbonate species/$H_2O_2$ process is suitable for the dechlorination−hydroxylation of chlorpyrazine. The difference in dechlorination performance between Cl−Py and Cl−Pa could be ascribed to the difference in electron density distribution between the pyridine ring and the pyrazine ring, thereby affecting N-oxidation and nucleophilic dechlorination processes.[61] Thus, the satisfactory dehalogenation performance of the carbonate species/$H_2O_2$ process ensures its practicability in water treatment.

## ■ ENVIRONMENTAL IMPLICATIONS

The production of chloropyridines reaches as high as several million tons per year. Chloropyridines easily enter the environment through industrial activities associated with pharmaceutical and chemical synthesis. Dechlorination of chloropyridines generally can reduce the threat to ecosystems and human health. However, the existing dechlorination technology is limited by the uncontrollable nonselective species, making it hard to effectively break the C−Cl bond of chloropyridines. To overcome this problem, we propose the carbonate species/$H_2O_2$ process based on the cooperation of a selective oxidant ($HCO_4^-$) and a selective reductant ($HO_2^-$) to precisely control the oxidation and reduction coupling reaction, thereby facilitating the cleavage of the C−Cl bond of Cl−Py. The high-efficient dechlorination efficiency of Cl−Py has been observed and confirmed in the carbonate species/$H_2O_2$ process. $HCO_4^-$- and $HO_2^-$-co-mediated pyridine N-oxidation−nucleophilic dechlorination coupling pathway of Cl−Py has been elucidated. The calculation and experimental results further clarify that pyridine N-oxidation of Cl−Py can effectively reduce the energy barrier of the dechlorination process. Besides, the formation of a nontoxic product is achieved in the carbonate species/$H_2O_2$ process. Moreover, the superiorities of the carbonate species/$H_2O_2$ process in terms of electric energy consumption and practical application are determined compared to the reported processes. Furthermore, the multiple advantages show an environmentally friendly prospect of the carbonate species/$H_2O_2$ process, such as the utilization of relatively inexpensive and nonpolluting $H_2O_2$, the stable and recyclable catalyst (bicarbonate or carbonate), easy operation, and without producing secondary pollution. Overall, the carbonate species/$H_2O_2$ process offers a promising avenue for the effective detoxification of wastewater containing halogenated organics, which is of both scientific and economic significance.

Although the carbonate species/$H_2O_2$ process requires a high dosage of $H_2O_2$ to ensure the reaction between substrates and reactive species, many bifunctional acid−base cooperative catalysts (such as nitrogen-doped carbon materials) have been developed to simultaneously activate substrates and reactive species.[62−64] Therefore, strategies such as adding nitrogen-doped carbon materials could be applied to reduce the dosage of $H_2O_2$ and promote the dehalogenation efficiency of halogenated organics in the carbonate species/$H_2O_2$ process, which needs further investigation. The carbonate species/$H_2O_2$ process is suitable for the treatment of industrial wastewater containing halogenated organics. As shown in Figure S22, Cl−Py in real industrial wastewater was significantly degraded after treatment by the carbonate species/$H_2O_2$ process. The residual carbonate species can be accommodated and disposed of within the subsequent physicochemical treatment process (such as chemical deposition).[28] Before its discharge into natural waters, this wastewater requires further treatment to comply with the discharge limit of carbonate discharge. The results of this study could also provide a fundamental understanding of the highly efficient utilization of the carbonate species/$H_2O_2$ process.

## ■ ASSOCIATED CONTENT

### Supporting Information

The Supporting Information is available free of charge at https://pubs.acs.org/doi/10.1021/acs.est.3c09878.

Chemicals and reagents; analytical methods of contaminant and its degradation intermediates and products; calculation of dehalogenation efficiency; experiments details on $^{13}C$ NMR spectral analysis and ESR analysis; quantification of reactive species; electrical energy consumption calculation method; toxicity assessment of Cl−Py and its degradation intermediates and products; DFT calculation methods; influence of $[\text{carbonate species}]_0/[H_2O_2]_0$ on Cl−Py removal; pH effect on Cl−Py removal and Cl−Py dechlorination; $^{13}C$ NMR spectra of $HCO_4^-$; equilibrium acid−base speciation of carbonate species; radical quenching results; ESR spectra of active species; changes in EIC peak area and concentration of Cl−Py−N-oxide and OH−Py−N-oxide; mass spectra of OH−Py and HOO−Py−N-oxide; degradation pathway of Cl−Py under different pH conditions; comparison on ESP distribution between Cl−Py and Cl−Py−N-oxide; dechlorination efficiency of Cl−Py−N-oxide by $HO_2^-$ alone; treatment of real Cl−Py wastewater; Cl−Py dechlorination efficiency in the additional experiment; and degradation of halogenated pyridines by $HO_2^-$ or $HCO_4^-$ alone. (PDF)

## ■ AUTHOR INFORMATION

### Corresponding Authors

**Jian-Ping Zou** − *National-Local Joint Engineering Research Center of Heavy Metals Pollutants Control and Resource Utilization, School of Environmental and Chemical Engineering, Nanchang Hangkong University, Nanchang 330063, P. R. China; Key Laboratory of Poyang Lake Environment and Resource Utilization, Ministry of Education, School of Resources & Environment, Nanchang University, Nanchang 330031, P. R. China;* orcid.org/0000-0002-3585-6541; Email: zjp_112@126.com

**Daishe Wu** − *Key Laboratory of Poyang Lake Environment and Resource Utilization, Ministry of Education, School of*



https://doi.org/10.1021/acs.est.3c09878
Environ. Sci. Technol. 2024, 58, 4438−4449

Resources & Environment, Nanchang University, Nanchang 330031, P. R. China; School of Materials and Chemical Engineering, Pingxiang University, Pingxiang 337000, P. R. China; Email: dswu@ncu.edu.cn

### Authors

**Ying Chen** − *National-Local Joint Engineering Research Center of Heavy Metals Pollutants Control and Resource Utilization, School of Environmental and Chemical Engineering, Nanchang Hangkong University, Nanchang 330063, P. R. China; Key Laboratory of Poyang Lake Environment and Resource Utilization, Ministry of Education, School of Resources & Environment, Nanchang University, Nanchang 330031, P. R. China*

**Lei Tian** − *National-Local Joint Engineering Research Center of Heavy Metals Pollutants Control and Resource Utilization, School of Environmental and Chemical Engineering, Nanchang Hangkong University, Nanchang 330063, P. R. China*

**Wen Liu** − *The Key Laboratory of Water and Sediment Sciences (Ministry of Education), College of Environmental Sciences and Engineering, Peking University, Beijing 100871, P. R. China;* orcid.org/0000-0002-6787-2431

**Yi Mei** − *National-Local Joint Engineering Research Center of Heavy Metals Pollutants Control and Resource Utilization, School of Environmental and Chemical Engineering, Nanchang Hangkong University, Nanchang 330063, P. R. China*

**Qiu-Ju Xing** − *National-Local Joint Engineering Research Center of Heavy Metals Pollutants Control and Resource Utilization, School of Environmental and Chemical Engineering, Nanchang Hangkong University, Nanchang 330063, P. R. China*

**Yi Mu** − *National-Local Joint Engineering Research Center of Heavy Metals Pollutants Control and Resource Utilization, School of Environmental and Chemical Engineering, Nanchang Hangkong University, Nanchang 330063, P. R. China;* orcid.org/0000-0001-9176-5049

**Ling-Ling Zheng** − *National-Local Joint Engineering Research Center of Heavy Metals Pollutants Control and Resource Utilization, School of Environmental and Chemical Engineering, Nanchang Hangkong University, Nanchang 330063, P. R. China*

**Qian Fu** − *National-Local Joint Engineering Research Center of Heavy Metals Pollutants Control and Resource Utilization, School of Environmental and Chemical Engineering, Nanchang Hangkong University, Nanchang 330063, P. R. China*

Complete contact information is available at: https://pubs.acs.org/10.1021/acs.est.3c09878

### Notes

The authors declare no competing financial interest.

## ■ ACKNOWLEDGMENTS

This work was supported by the National Science Foundation of China (52170082, 51938007, and 21906076) and the Natural Science Foundation of Jiangxi Province (20212ACB203008).

## ■ REFERENCES

(1) Yang, X. R.; Ding, X.; Zhou, L.; Fan, H. H.; Wang, X. B.; Ferronato, C.; Chovelon, J. M.; Xiu, G. L. New insights into clopyralid degradation by sulfate radical: Pyridine ring cleavage pathways. *Water Res.* **2020**, *171*, 115378−115387.

(2) Jiang, X. B.; Shen, J. Y.; Xu, K. C.; Chen, D.; Mu, Y.; Sun, X. Y.; Han, W. Q.; Li, J. S.; Wang, L. J. Substantial enhancement of anaerobic pyridine bio-mineralization by electrical stimulation. *Water Res.* **2018**, *130*, 291−299.

(3) Min, Y.; Zhou, X.; Chen, J. J.; Chen, W. X.; Zhou, F. Y.; Wang, Z. Y.; Yang, J.; Xiong, C.; Wang, Y.; Li, F. T.; Yu, H. Q.; Wu, Y. Integrating single-cobalt-site and electric field of boron nitride in dechlorination electrocatalysts by bioinspired design. *Nat. Commun.* **2021**, *12*, 303 DOI: 10.1038/s41467-020-20619-w.

(4) Yu, W. T.; Jiang, H.; Fang, J. H.; Song, S. Designing an electron-deficient Pd/$NiCo_2O_4$ bifunctional electrocatalyst with an enhanced hydrodechlorination activity to reduce the consumption of Pd. *Environ. Sci. Technol.* **2021**, *55*, 10087−10096.

(5) Huang, D. H.; Kim, D. J.; Rigby, K.; Zhou, X. C.; Wu, X. H.; Meese, A.; Niu, J. F.; Stavitski, E.; Kim, J. H. Elucidating the role of single-atom Pd for electrocatalytic hydrodechlorination. *Environ. Sci. Technol.* **2021**, *55*, 13306−13316.

(6) Krzemińska, A.; Paneth, P. DFT studies of $S_N2$ dechlorination of polychlorinated biphenyls. *Environ. Sci. Technol.* **2016**, *50*, 6293−6298.

(7) Lian, F.; Xu, K.; Zeng, C. C. The synergism of sequential paired electrosynthesis with halogen bonding activation for the cyclization of organochlorides with olefins. *Sci. China: Chem.* **2023**, *66*, 540−547.

(8) Martin, E. T.; McGuire, C. M.; Mubarak, M. S.; Peters, D. G. Electroreductive remediation of halogenated environmental pollutants. *Chem. Rev.* **2016**, *116*, 15198−15234.

(9) Min, Y.; Zhou, X.; Chen, J. J.; Chen, W. X.; Zhou, F. Y.; Wang, Z. Y.; Yang, J.; Xiong, C.; Wang, Y.; Li, F. T.; Yu, H. Q.; Wu, Y. Integrating single-cobalt-site and electric field of boron nitride in dechlorination electrocatalysts by bioinspired design. *Nat. Commun.* **2021**, *12*, 303 DOI: 10.1038/s41467-020-20619-w.

(10) Mitoma, Y.; Nagashima, S.; Simion, C.; Simion, A. M.; Yamada, T.; Mimura, K.; Ishimoto, K.; Tashiro, M. Dehalogenation of aromatic halides using metallic calcium in ethanol. *Environ. Sci. Technol.* **2001**, *35*, 4145−4148.

(11) Zhang, J.; Ji, Q. H.; Lan, H. C.; Zhang, G.; Liu, H. J.; Qu, J. H. Synchronous reduction−oxidation process for efficient removal of trichloroacetic acid: H* initiates dechlorination and •OH is responsible for removal efficiency. *Environ. Sci. Technol.* **2019**, *53*, 14586−14594.

(12) Shen, X. Q.; Xiao, F.; Zhao, H. Y.; Chen, Y.; Fang, C.; Xiao, R.; Chu, W. H.; Zhao, G. H. In situ-formed PdFe nanoalloy and carbon defects in cathode for synergic reduction−oxidation of chlorinated pollutants in electro-Fenton process. *Environ. Sci. Technol.* **2020**, *54*, 4564−4572.

(13) Li, S. P.; Liu, C. L.; Lv, W. Y.; Liu, G. G. Incorporating oxygen atoms in a $SnS_2$ atomic layer to simultaneously stabilize atomic hydrogen and accelerate the generation of hydroxyl radicals for water decontamination. *Environ. Sci. Technol.* **2022**, *56*, 4980−4987.

(14) Li, N.; Song, X. Z.; Wang, L.; Geng, X. L.; Wang, H.; Tang, H. Y.; Bian, Z. Y. Single-atom cobalt catalysts for electrocatalytic hydrodechlorination and oxygen reduction reaction for the degradation of chlorinated organic compounds. *ACS Appl. Mater. Interfaces* **2020**, *12*, 24019−24029.

(15) Wei, K.; Wan, Y. Y.; Liao, M. Z.; Cao, S. Y.; Zhang, H.; Peng, X.; Gu, H. Y.; Ling, C. C.; Li, M. Q.; Shi, Y. B.; Ai, Z. H.; Gong, J. M.; Zhang, L. Z. A controllable reduction-oxidation coupling process for chloronitrobenzenes remediation: From lab to field trial. *Water Res.* **2022**, *218*, 118453−118461.

(16) Li, Y.; Miller, C. J.; Wu, L.; Waite, T. D. Hydroxyl radical production via a reaction of electrochemically generated hydrogen peroxide and atomic hydrogen: an effective process for contaminant oxidation? *Environ. Sci. Technol.* **2022**, *56*, 5820−5829.

(17) Zeng, H. B.; Zhang, G.; Ji, Q. H.; Liu, H. J.; Hua, X.; Xia, H. L.; Sillanpää, M.; Qu, J. H. pH-independent production of hydroxyl radical from atomic H*-mediated electrocatalytic $H_2O_2$ reduction: A

green Fenton process without byproducts. *Environ. Sci. Technol.* **2020**, *54*, 14725−14731.
(18) Gu, Z.; Zhang, Z. Y.; Ni, N.; Hu, C. Z.; Qu, J. H. Simultaneous phenol removal and resource recovery from phenolic wastewater by electrocatalytic hydrogenation. *Environ. Sci. Technol.* **2022**, *56*, 4356−4366.
(19) Zheng, W. T.; Liu, Y. B.; Liu, F. Q.; Wang, Y.; Ren, N. Q.; You, S. J. Atomic hydrogen in electrocatalytic systems: Generation, identification, and environmental applications. *Water Res.* **2022**, *223*, 118994−119009.
(20) Bokare, A. D.; Choi, W. Y. Bicarbonate-induced activation of $H_2O_2$ for metal-free oxidative desulfurization. *J. Hazard. Mater.* **2016**, *304*, 313−319.
(21) Pan, H. P.; Gao, Y.; Li, N.; Zhou, Y.; Lin, Q. T.; Jiang, J. Recent advances in bicarbonate-activated hydrogen peroxide system for water treatment. *Chem. Eng. J.* **2021**, *408*, 127332−127344.
(22) Mu, Y.; Chen, Y.; Fu, Q.; He, P. Y.; Sun, Q.; Zou, J. P.; Zhang, L. Z.; Wang, D. K.; Luo, S. L. Transformation of atrazine to hydroxyatrazine with alkali-$H_2O_2$ treatment: An efficient dechlorination strategy under alkaline conditions. *ACS EST Water* **2021**, *1*, 1868−1877.
(23) Hansen, T.; Vermeeren, P.; Bickelhaupt, F. M.; Hamlin, T. A. Origin of the $\alpha$-effect in $S_N2$ reactions. *Angew. Chem., Int. Ed.* **2021**, *60*, 20840−20848.
(24) Zhao, S. P.; Xi, H. L.; Zuo, Y. J.; Wang, Q.; Wang, Z. C.; Yan, Z. Y. Bicarbonate-activated hydrogen peroxide and efficient decontamination of toxic sulfur mustard and nerve gas simulants. *J. Hazard. Mater.* **2018**, *344*, 136−145.
(25) Bakhmutova-Albert, E. V.; Yao, H. R.; Denevan, D. E.; Richardson, D. E. Kinetics and mechanism of peroxymonocarbonate formation. *Inorg. Chem.* **2010**, *49*, 11287−11296.
(26) Puiu, M.; Galaon, T.; Bondilă, L.; Răducan, A.; Oancea, D. Feed-back action of nitrite in the oxidation of nitrophenols by bicarbonate-activated peroxide system. *Appl. Catal., A* **2016**, *516*, 90−99, DOI: 10.1016/j.apcata.2016.02.021.
(27) Yao, H. R.; Richardson, D. E. Bicarbonate surfoxidants: Micellar oxidations of aryl sulfides with bicarbonate-activated hydrogen peroxide. *J. Am. Chem. Soc.* **2003**, *125*, 6211−6221.
(28) Chen, Y.; Mu, Y.; Tian, L.; Zheng, L. L.; Mei, Y.; Xing, Q. J.; Liu, W.; Zou, J. P.; Yang, L. X.; Luo, S. L.; Wu, D. S. Targeted decomplexation of metal complexes for efficient metal recovery by ozone/percarbonate. *Environ. Sci. Technol.* **2023**, *57*, 5034−5045.
(29) Lu, Z. Y.; Chen, G. X.; Siahrostami, S.; Chen, Z. H.; Liu, K.; Xie, J.; Liao, L.; Wu, T.; Lin, D. C.; Liu, Y. Y.; Jaramillo, T. F.; Nørskov, J. K.; Cui, Y. High-efficiency oxygen reduction to hydrogen peroxide catalysed by oxidized carbon materials. *Nat. Catal.* **2018**, *1*, 156−162.
(30) Becke, A. D. Density-functional thermochemistry. III. The role of exact exchange. *J. Chem. Phys.* **1993**, *98*, 5648−5652.
(31) Lee, C.; Yang, W.; Parr, R. G. Development of the Colle-Salvetti correlation-energy formula into a functional of the electron density. *Phys. Rev. B* **1988**, *37*, 785−789.
(32) Grimme, S.; Stephan, E.; Lars, G. Effect of the damping function in dispersion corrected density functional theory. *J. Comput. Chem.* **2011**, *32*, 1456−1465.
(33) Weigend, F.; Ahlrichs, R. Balanced basis sets of split valence, triple zeta valence and quadruple zeta valence quality for H to Rn: Design and assessment of accuracy. *Phys. Chem. Chem. Phys.* **2005**, *7*, 3297−3305.
(34) Weigend, F. Accurate coulomb-fitting basis sets for H to Rn. *Phys. Chem. Chem. Phys.* **2006**, *8*, 1057−1065.
(35) Yang, X. J.; Duan, Y. H.; Wang, J. L.; Wang, H. L.; Liu, H. L.; Sedlak, D. L. Impact of peroxymonocarbonate on the transformation of organic contaminants during hydrogen peroxide in situ chemical oxidation. *Environ. Sci. Technol. Lett.* **2019**, *6*, 781−786.
(36) Mani, F.; Peruzzini, M.; Stoppioni, P. CO2 absorption by aqueous NH3 solutions: speciation of ammonium carbamate, bicarbonate and carbonate by a 13C NMR study. *Green Chem.* **2006**, *8*, 995−1000.
(37) Li, Y. J.; Dong, H. R.; Xiao, J. Y.; Li, L.; Chu, D. D.; Hou, X. Z.; Xiang, S. X.; Dong, Q. X.; Zhang, H. X. Advanced oxidation processes for water purification using percarbonate: Insights into oxidation mechanisms, challenges, and enhancing strategies. *J. Hazard. Mater.* **2023**, *442*, 130014−130029.
(38) Shi, Y. B.; Yang, Z. P.; Shi, L. J.; Li, H.; Liu, X. P.; Zhang, X.; Cheng, J. D.; Liang, C.; Cao, S. Y.; Guo, F. R.; Liu, X.; Ai, Z. H.; Zhang, L. Z. Surface boronizing can weaken the excitonic effects of BiOBr nanosheets for efficient $O_2$ activation and selective NO oxidation under visible light irradiation. *Environ. Sci. Technol.* **2022**, *56*, 14478−14486.
(39) Balagam, B.; Richardson, D. E. The mechanism of carbon dioxide catalysis in the hydrogen peroxide N-oxidation of amines. *Inorg. Chem.* **2008**, *47*, 1173−1178.
(40) Richardson, D. E.; Yao, H. R.; Frank, K. M.; Bennett, D. A. Equilibria, kinetics, and mechanism in the bicarbonate activation of hydrogen peroxide: Oxidation of sulfides by peroxymonocarbonate. *J. Am. Chem. Soc.* **2000**, *122*, 1729−1739.
(41) Ling, L.; Sun, J. L.; Fang, J. Y.; Shang, C. Kinetics and mechanisms of degradation of chloroacetonitriles by the UV/$H_2O_2$ process. *Water Res.* **2016**, *99*, 209−215.
(42) Wang, W. H.; Wang, Y. H.; Feng, W. L.; Wang, W. L.; Li, P. Theoretical investigations on the reactivity of hydrogen peroxide toward 2,3,7,8-tetrachlorodibenzo-p-dioxin. *Molecules* **2018**, *23*, 2826−2839.
(43) Kang, Q. K.; Lin, Y. Z.; Li, Y. T.; Xu, L.; Li, K.; Shi, H. Catalytic $S_NAr$ hydroxylation and alkoxylation of aryl fluorides. *Angew. Chem., Int. Ed.* **2021**, *60*, 20391−20399.
(44) Tay, N. E. S.; Nicewicz, D. A. Cation radical accelerated nucleophilic aromatic substitution via organic photoredox catalysis. *J. Am. Chem. Soc.* **2017**, *139*, 16100−16104.
(45) Rohrbach, S.; Smith, A. J.; Pang, J. H.; Poole, D. L.; Tuttle, T.; Chiba, S.; Murphy, J. A. Concerted nucleophilic aromatic substitution reactions. *Angew. Chem., Int. Ed.* **2019**, *58*, 16368−16388.
(46) Mitchell, S. M.; Ahmad, M.; Teel, A. L.; Watts, R. J. Degradation of perfluorooctanoic acid by reactive species generated through catalyzed $H_2O_2$ propagation reactions. *Environ. Sci. Technol. Lett.* **2014**, *1*, 117−121.
(47) Zhang, B. T.; Kuang, L. L.; Teng, Y. G.; Fan, M. H.; Ma, Y. Application of percarbonate and peroxymonocarbonate in decontamination technologies. *J. Environ. Sci.* **2021**, *105*, 100−115.
(48) Cai, Y. H.; Luo, Y. H.; Long, X. X.; Roldan, M. A.; Yang, S. Z.; Zhou, C.; Zhou, D. D.; Rittmann, B. E. Reductive Dehalogenation of Herbicides Catalyzed by Pd0NPs in a H2-Based Membrane Catalyst-Film Reactor. *Environ. Sci. Technol.* **2022**, *56*, 18030−18040.
(49) Jing, K.; Kong, D. Y.; Lu, J. H. Change of disinfection byproducts formation potential of natural organic matter after exposure to persulphate and bicarbonate. *Water Res.* **2020**, *182*, 115970−115977.
(50) Moreno, J. M.; Aramendía, M. A.; Marinas, A.; Marinas, J. M.; Urbano, F. J. Individual and competitive liquid-phase hydrodechlorination of chlorinated pyridines over alkali-modified Pd/$ZrO_2$. *Appl. Catal., B* **2007**, *76*, 34−41.
(51) Raut, S. S.; Kamble, S. P.; Kulkarni, P. S. Efficacy of zero-valent copper ($Cu^0$) nanoparticles and reducing agents for dechlorination of mono chloroaromatics. *Chemosphere* **2016**, *159*, 359−366.
(52) He, L.; Ji, Y. X.; Cheng, J.; Wang, C. R.; Jiang, L. X.; Chen, X. Y.; Li, H. Y.; Ke, S.; Wang, J. B. Effect of pH and Cl- concentration on the electrochemical oxidation of pyridine in low-salinity reverse osmosis concentrate: Kinetics, mechanism, and toxicity assessment. *Chem. Eng. J.* **2022**, *449*, 137669−137678.
(53) Yang, X. R.; Cao, X.; Zhang, L.; Wu, Y. L.; Zhou, L.; Xiu, G. L.; Ferronato, C.; Chovelon, J. M. Sulfate radical-based oxidation of the aminopyralid and picloram herbicides: The role of amino group on pyridine ring. *J. Hazard. Mater.* **2021**, *405*, 124181−124190.
(54) Mao, R.; Huang, C.; Zhao, X.; Ma, M.; Qu, J. H. Dechlorination of triclosan by enhanced atomic hydrogen-mediated electrochemical reduction: Kinetics, mechanism, and toxicity assessment. *Appl. Catal., B* **2019**, *241*, 120−129.


https://doi.org/10.1021/acs.est.3c09878
*Environ. Sci. Technol.* 2024, 58, 4438−4449

(55) Liu, X. Y.; Chen, L.; Yang, M. T.; Tan, C. Q.; Chu, W. H. The occurrence, characteristics, transformation and control of aromatic disinfection by-products: A review. *Water Res.* **2020**, *184*, 116076−116090.
(56) Shi, H. F.; Jiang, X. B.; Chen, D.; Li, Y.; Hou, C.; Wang, L. J.; Shen, J. Y. $BiVO_4$/FeOOH semiconductor-microbe interface for enhanced visible-light-driven biodegradation of pyridine. *Water Res.* **2020**, *187*, 116464−116474.
(57) Sadowsky, D.; McNeill, K.; Cramer, C. J. Dehalogenation of aromatics by nucleophilic aromatic substitution. *Environ. Sci. Technol.* **2014**, *48*, 10904−10911.
(58) Lippa, K. A.; Roberts, A. L. Nucleophilic aromatic substitution reactions of chloroazines with bisulfide ($HS^-$) and polysulfides ($Sn^{2-}$). *Environ. Sci. Technol.* **2002**, *36*, 2008−2018.
(59) Sadowsky, D.; McNeill, K.; Cramer, C. J. Thermochemical factors affecting the dehalogenation of aromatics. *Environ. Sci. Technol.* **2013**, *47*, 14194−14203.
(60) Lippa, K. A.; Roberts, A. L. Nucleophilic aromatic substitution reactions of chloroazines with bisulfide ($HS^-$) and polysulfides ($Sn^{2-}$). *Environ. Sci. Technol.* **2002**, *36*, 2008−2018.
(61) Tekle-Röttering, A.; Reisz, E.; Jewell, K. S.; Lutze, H. V.; Ternes, T. A.; Schmidt, W.; Schmidt, T. C. Ozonation of pyridine and other N-heterocyclic aromatic compounds: Kinetics, stoichiometry, identification of products and elucidation of pathways. *Water Res.* **2016**, *102*, 582−593.
(62) Ding, L. Z.; Zhang, P. P.; Luo, H.; Hu, Y. F.; Banis, M. N.; Yuan, X. L.; Liu, N. Nitrogen-doped carbon materials as metal-free catalyst for the dechlorination of trichloroethylene by sulfide. *Environ. Sci. Technol.* **2018**, *52*, 14286−14293.
(63) Wang, J. J.; Liu, Z. W.; Li, S. Y.; Li, C. P.; Liu, S.; Feng, J. W.; Tan, R. Foam-like boron-doped g-$C_3N_4$ as acid-base cooperative catalyst for efficient nucleophilic addition in water. *Green Chem. Eng.* **2021**, *2*, 239−249.
(64) Ding, L. Z.; Wang, Y. H.; Tong, L. Z.; Liu, N.; Wang, C.; Hu, Q. N-doped biochar-catalyzed dechlorination of carbon tetrachloride in sulfide-containing aqueous solutions: Performances, mechanisms and pathways. *Water Res.* **2022**, *223*, 119006−119016.


https://doi.org/10.1021/acs.est.3c09878
*Environ. Sci. Technol.* 2024, 58, 4438−4449